

# An a priori solar radiation pressure model for the QZSS Michibiki satellite

Qile Zhao<sup>1,2</sup> · Guo Chen<sup>1,3</sup> · Jing Guo<sup>1,4</sup>  · Jingnan Liu<sup>1,2</sup> · Xianglin Liu<sup>5</sup>

Received: 4 July 2016 / Accepted: 4 July 2017 / Published online: 14 July 2017  
© Springer-Verlag GmbH Germany 2017

**Abstract** It has been noted that the satellite laser ranging (SLR) residuals of the Quasi-Zenith Satellite System (QZSS) Michibiki satellite orbits show very marked dependence on the elevation angle of the Sun above the orbital plane (i.e., the  $\beta$  angle). It is well recognized that the systematic error is caused by mismodeling of the solar radiation pressure (SRP). Although the error can be reduced by the updated ECOM SRP model, the orbit error is still very large when the satellite switches to orbit-normal (ON) orientation. In this study, an a priori SRP model was established for the QZSS Michibiki satellite to enhance the ECOM model. This model is expressed in ECOM's  $D$ ,  $Y$ , and  $B$  axes (DYB) using seven parameters for the yaw-steering (YS) mode, and additional three parameters are used to compensate the remaining modeling deficiencies, particularly the perturbations in the  $Y$  axis, based on a redefined DYB for the ON mode. With the proposed a priori model, QZSS Michibiki's precise orbits over 21 months were determined. SLR validation indicated that the systematic  $\beta$ -angle-dependent error was reduced when the satellite was in the YS mode, and better than an 8-cm root mean square (RMS) was achieved. More importantly, the

orbit quality was also improved significantly when the satellite was in the ON mode. Relative to ECOM and adjustable box-wing model, the proposed SRP model showed the best performance in the ON mode, and the RMS of the SLR residuals was better than 15 cm, which was a two times improvement over the ECOM without a priori model used, but was still two times worse than the YS mode.

**Keywords** QZSS Michibiki · Solar radiation pressure · Precise orbit determination · MGEX · Yaw-steering attitude · Orbit-normal attitude

## 1 Introduction

The Quasi-Zenith Satellite System (QZSS) is a regional navigation satellite system being developed by the Japan Aerospace Exploration Agency (JAXA) to provide GPS-compatible signals as well as integrity and correction information for users in the Asia–Pacific region (Inaba et al. 2009). The system will consist of three inclined geosynchronous orbit (IGSO) satellites and one geostationary (GEO) satellite by 2018; the first IGSO satellite, Michibiki, was launched on September 11, 2010.

Precise orbit determination (POD) for the QZSS Michibiki satellite is essential for high-precision positioning with QZSS signals and for improving navigation performance. Because this satellite carries a laser retro-reflector array (LRA), satellite laser ranging (SLR) measurements collected by the International Laser Ranging Service (ILRS) (Pearlman et al. 2002) can be used to determine its orbits and to independently assess the quality of POD solutions based on Global Navigation Satellite System (GNSS) microwave observations. One of the earlier POD results for Michibiki was based solely on SLR measurements. The accuracy in the radial direction was 20 cm (Akiyama and Otsubo 2012). Another study of QZSS

✉ Jing Guo  
jingguo@whu.edu.cn

<sup>1</sup> GNSS Research Center, Wuhan University,  
No. 129 Luoyu Road, Wuhan 430079, China

<sup>2</sup> Collaborative Innovation Center of Geospatial Technology,  
Wuhan University, No. 129 Luoyu Road, Wuhan 430079,  
China

<sup>3</sup> School of Geodesy and Geomatics, Wuhan University,  
No. 129 Luoyu Road, Wuhan 430079, China

<sup>4</sup> School of Civil Engineering and Geosciences, Newcastle  
University, Newcastle upon Tyne NE1 7RU, UK

<sup>5</sup> Fugro Intersite B.V., 2263 HW Leidschendam,  
The Netherlands

satellite POD used the data of five GNSS tracking stations of the Cooperative Network for GIOVE Observation (CONGO) from day of year (DOY) 173 to 250, 2011 (Steigenberger et al. 2013). The SLR validation demonstrated that the accuracy of the best orbit solution reached approximately 32.5 cm. The corresponding day-boundary discontinuity was approximately 16.4 cm. With more ground tracking stations, Takasu (2013) demonstrated that the 3D root mean square (RMS) of 24-h overlapping orbit differences (OODs) reached 5.99 cm from his POD results for DOY 155 to 305, 2011. However, systematic errors in orbits were not demonstrated in those studies, probably because none of them used greater than half-year orbits. Thanks to the efforts of the International GNSS Service (IGS) (Dow et al. 2009) Multi-GNSS Experiment (MGEX) (Montenbruck et al. 2014), greater than 2-year Michibiki precise ephemerides have been provided by Technische Universität München (TUM) in München, Germany, and by the JAXA. Steigenberger et al. (2014) compared and analyzed the approximately 1.5-year Michibiki orbits from those two analysis centers (ACs). The SLR residuals showed pronounced dependence on the elevation angle of the Sun above the orbital plane (i.e., the  $\beta$  angle). A  $\beta$ -angle-dependent systematic error also presents for Galileo orbits determined by the Extended Center for orbit determination in Europe Orbit Model (ECOM) (Beutler et al. 1994). The SLR residuals of Galileo orbits showed a pronounced “bow-tie” pattern and reached the “tie” when the  $|\beta|$  angle was close to the maximum value. The dependence of the orbit error on the  $\beta$  angle is obviously related to the SRP modeling. To reduce the deficiency of the ECOM for the Galileo POD, Montenbruck et al. (2015) established an a priori SRP model based on a generic box-wing model in yaw-steering (YS) mode to augment the ECOM. The reason for that type of model is that Galileo satellites have a markedly elongated shape instead of a cubic one as well as a large area-to-mass ratio. Michibiki also has similar features.

Besides the inability of the ECOM to properly describe SRP acceleration acting on a stretched body with a large area-to-mass ratio, Michibiki’s attitude control mode makes the POD more complicated. Similar to IGSO and medium earth orbit (MEO) satellites of the Chinese BeiDou Navigation Satellite System (BDS), Michibiki uses two attitude modes, namely the YS and the orbit-normal (ON) modes. The transition of the Michibiki attitude from YS to ON mode, and vice versa, takes place at a nominal  $|\beta|$ -angle threshold of approximately  $20^\circ$  (Ishijima et al. 2008). However, Hauschild et al. (2012) showed that the transition between the YS and ON modes did not take place at exactly the nominal  $|\beta|$ -angle threshold, but was typically done at a convenient nearby epoch when the yaw angles in the YS and ON modes differed the least. A comparison between IGS MGEX JAXA and TUM QZSS orbits demonstrated marked accuracy degradation when the satellites switched to the ON orientation. The

orbit differences in ON mode showed a pronounced “bow-tie” pattern in radial direction and linear dependence with respect to the  $\beta$  angle in the cross-track component in 2013 (Steigenberger et al. 2014). Although the orbit consistency improved in 2014, accuracy degradation was still observed. This clearly reflected the deficiency of the ECOM for POD in the ON mode. A similar deficiency was reported for BDS IGSO and MEO satellites by Guo et al. (2013). To overcome the problem of Michibiki satellite an a priori SRP model was established to augment the ECOM, and the  $\beta$ -dependent a priori values for 9 parameters in the ECOM were estimated with rather long-period data. In addition, Ikari et al. (2013) modified the box-wing model to account for the forces caused by the larger L-band antenna in the nadir direction and proposed a box-wing-hat model. However, the orbits determined by the box-wing-hat model showed a lower performance with respect to that determined by the ECOM with an a priori model (Ikari et al. 2013).

The ECOM models could introduce large draconitic error in GNSS geodetic products (Meindl et al. 2013; Rodríguez-Solano et al. 2014). To reduce the error in the time series of IGS products, Arnold et al. (2015) proposed an updated ECOM model (ECOM2). Although the dependency of SLR residuals on  $\beta$ -angle was reduced with ECOM2 model in YS mode, clear parabolic variations with respect to  $\beta$ -angle still exist in ON mode (Prange et al. 2015, 2017). This indicates that the ECOM2 model was still deficient for POD in the ON mode, because it is designed for satellites in YS mode and inadequate to model the SRP when satellites are in eclipse seasons or in non-yaw-steering attitude modes. Guo et al. (2013) improved the orbit quality for BDS IGSO and MEO satellites in the ON mode by introducing into the ECOM a constant acceleration bias in the along-track. SLR validation and OODs confirmed a substantial improvement. However, the applicability of this approach to the Michibiki satellite has not been checked.

The present study focuses on SRP modeling of the QZSS Michibiki satellite in both YS and ON modes. The proposed SRP model aims to reduce the  $\beta$ -angle-dependent error in the YS mode and overcome the deficiencies of the ECOM and ECOM2 in the ON mode. This paper is organized as follows. Section 2 presents the GNSS SRP models; the ECOM and its reduced 5-parameter version (ECOM1) as well as ECOM2 are introduced and clarified, and the box-wing model and its reformulation are illustrated for further comparison and application. In Sect. 3, the performance of these models for Michibiki POD is compared and analyzed. Based on these results, an a priori model to augment the ECOM is established and refined in Sect. 4. The coefficients of the a priori model are fitted to real QZSS measurements in 2014 that cover the full range of the Sun elevation. In addition, the model is validated further with the first 9 months of 2015. Finally, this study is summarized and concluded in Sect. 5.

## 2 SRP models for GNSS satellites

For GNSS satellites, particularly for IGSO satellites, SRP is the main non-conservative orbit perturbation. SRP acting on a satellite is difficult to model due to perturbed acceleration that depends on the physical and geometrical properties of the satellite and its orientation with respect to the incidence radiation. Currently, several models have been proposed to model SRP acting on GNSS satellites; they could be classified into three types: (1) empirical models; that is, the ECOM, ECOM1, and ECOM2 (Beutler et al. 1994; Springer et al. 1999; Arnold et al. 2015). These models can best fit the real GNSS tracking data, though they do not consider actual physical forces acting on the satellite. (2) Analytical models based on the physical and geometrical properties of the satellite; that is, ROCK models (Fliegel et al. 1992; Fliegel and Gallini 1996). The main disadvantage of these models is that changes in the a priori geometrical or optical properties of a satellite, or attitude deviations from the nominal, result in deficiencies in modeling perturbed accelerations. (3) Semi-analytical and semi-empirical models; that is, the adjustable box-wing model (ABW) (Rodríguez-Solano et al. 2012) and the GPS Solar Pressure Model (GSPM) (Bar-Sever and Kuang 2004, 2005). Such models compromise the analytical SRP models as well as the empirical ones and could fit real tracking data well with a clear physical understanding of SRP. In this section, the ECOM models and the ABW model are presented for further discussion.

### 2.1 ECOM SRP models

To improve GPS orbit accuracy, the ECOM was developed in the 1990s (Beutler et al. 1994). The ECOM decomposes the perturbed acceleration into three orthogonal directions: the Sun direction ( $eD$ ), the solar panel axis ( $eY$ ), and the orthogonal axis ( $eB$ ). It adopts a truncated Fourier series expansion for each component using the angular argument  $\varphi$ . The total acceleration at 1 AU induced by SRP is expressed as

$$\mathbf{a} = \mathbf{a}_{\text{prior}} + D(\varphi) \mathbf{e}_D + Y(\varphi) \mathbf{e}_Y + B(\varphi) \mathbf{e}_B, \tag{1}$$

where  $\mathbf{a}_{\text{prior}}$  is the optional a priori SRP model. For ECOM and ECOM1 (Springer et al. 1999),  $\varphi$  is the satellite’s argument of the latitude, whereas for ECOM2 it is the difference of the satellite’s argument of the latitude and the Sun’s argument of the latitude. In addition, the three vectors  $\mathbf{e}_{D,YS}$ ,  $\mathbf{e}_{Y,YS}$ , and  $\mathbf{e}_{B,YS}$  span the DYB frame introduced by Beutler et al. (1994) for the YS attitude

$$\begin{aligned} \mathbf{e}_{D,YS} &= \mathbf{e}_\odot \\ \mathbf{e}_{Y,YS} &= \frac{\mathbf{e}_\odot \times \mathbf{r}}{\|\mathbf{e}_\odot \times \mathbf{r}\|}, \\ \mathbf{e}_{B,YS} &= \mathbf{e}_{D,YS} \times \mathbf{e}_{Y,YS} \end{aligned} \tag{2}$$

where  $\mathbf{e}_\odot$  is the unit vector of the Sun direction and  $\mathbf{r}$  is the geocentric vectors of the satellite. In Eq. (1),  $D(\varphi)$ ,  $Y(\varphi)$ , and  $B(\varphi)$  can be expanded as a truncated Fourier series

$$\begin{aligned} D(\varphi) &= D_0 + \sum_{i=1}^{n_D} \left\{ D_{i,c} \cos(C_j^D \varphi) + D_{i,s} \sin(S_j^D \varphi) \right\} \\ Y(\varphi) &= Y_0 + \sum_{i=1}^{n_Y} \left\{ Y_{i,c} \cos(C_j^Y \varphi) + Y_{i,s} \sin(S_j^Y \varphi) \right\}, \\ B(\varphi) &= B_0 + \sum_{i=1}^{n_B} \left\{ B_{i,c} \cos(C_j^B \varphi) + B_{i,s} \sin(S_j^B \varphi) \right\} \end{aligned} \tag{3}$$

where the upper limit values  $n_D$ ,  $n_Y$ , and  $n_B$  are defined by users, and  $C_j$  and  $S_j$  with different superscripts ( $D, Y, B$ ) are positive integers for cosine and sine components in each axis, respectively,  $D, Y$ , and  $B$  with different subscripts are the SRP coefficients to be estimated. For  $n_D = n_Y = n_B = 1$ , this model is the ECOM introduced by Beutler et al. (1994). In this case, the three constant terms  $D_0$ ,  $Y_0$ , and  $B_0$ , and up to 6 one-cycle-per-revolution terms ( $D_{1,c}$ ,  $D_{1,s}$ ,  $Y_{1,c}$ ,  $Y_{1,s}$ ,  $B_{1,c}$ , and  $B_{1,s}$ ) should be adjusted. For  $n_B = 1$  and  $n_D = n_Y = 0$ , the ECOM1 is obtained (Springer et al. 1999). For ECOM2, only even-order terms for the  $D(\varphi)$  and odd-order terms for the  $B(\varphi)$  components need to be considered (i.e.,  $n_Y = 0$ ,  $C_j^D = S_j^D = j = 2i$  and  $C_j^B = S_j^B = j = 2i - 1$ ). With massive tests, Arnold et al. (2015) suggested that  $n_D$  and  $n_B$  with no less than two values are preferred.

Originally, the analytical ROCK model furnished by Rockwell International was used as the a priori model for GPS. Later, Springer et al. (1999) presented an alternative a priori model derived by fitting a time series of estimated SRP parameters. Although the ECOM and ECOM1 model were developed for use with an a priori model, good performance can also be obtained without such a model. Hence, the purely empirical ECOM has been used by some IGS analysis centers to routine generate GPS and GLONASS orbits for a long time (see <ftp://igs.ign.fr/pub/igs/igscb/center/analysis/>). In addition, the model has been most widely adopted even for POD of the newly launched GNSS satellites due to the lack of alternative analytical SRP models. However, the model has problems sufficiently representing the orbits of Galileo satellites. The introduction of an a priori model to augment the ECOM1 has overcome the deficiency (Montenbruck et al. 2015).

### 2.2 The box-wing model

Following Milani et al. (1987), the SRP acceleration contributed by a surface of area  $A$  depends on the relative alignment of the Sun direction  $\mathbf{e}_\odot$  and the surface normal  $\mathbf{e}_N$  as well as the fraction of absorbed photons ( $\alpha$ ), of diffusely reflected photons ( $\delta$ ), and of specularly reflected photons ( $\rho$ ).

For  $\cos \theta = \mathbf{e}_\odot^T \cdot \mathbf{e}_N > 0$ , that is, for an illuminated surface, the acceleration at a distance of 1 AU can be accounted as

$$a = \frac{-A S_0}{M c} \cos \theta \left[ (1 - \rho) \mathbf{e}_\odot + 2 \left( \frac{\delta}{3} + \rho \cos \theta \right) \mathbf{e}_N \right]. \tag{4}$$

Here,  $S_0 = 1367 \text{ W/m}^2$  is the solar flux at 1AU,  $c$  is the vacuum velocity of light, and  $M$  is the total mass of the satellite. This equation can be used for SRP calculation on solar panels (SPs). For a satellite bus, which is covered by multilayer insulation for thermal protection, the thermal reradiation must be accounted for. Fliegel et al. (1992) presented a formulation of the thermal reradiated perturbations based on Lambert’s law. The modified formulation for the acceleration on the satellite bus surfaces is

$$a = \frac{-A S_0}{M c} \cos \theta \left[ (\alpha + \delta) \left( \mathbf{e}_\odot + \frac{2}{3} \mathbf{e}_N \right) + 2\rho \cos \theta \mathbf{e}_N \right]. \tag{5}$$

The box-wing model was originally developed for Topex/Poseidon POD (Marshall and Luthcke 1994). It presents the satellite as a box (satellite bus) and two wings (SPs); the acceleration acting on each surface can be calculated based on the physical model in an analytical way. Previously, this model was used mainly for low earth orbiters with only one scaling factor being estimated. Rodríguez-Solano et al. (2012) used this model for GNSS satellites and improved its performance through adjustment of the absorption plus diffuse reflection (AD) as well as the specular reflection (R) for illuminated satellite bus surfaces (+X, +Z, -Z), and optical properties of SPs, the empirical constant acceleration in Y axes (Y0), and the SP lag angle (SB). It is therefore called an ABW model. With this model, draconitic error in GNSS-derived geodetic products is reduced (Rodríguez-Solano et al. 2014) without loss of the orbit accuracy compared to that derived with the ECOM mode (Rodríguez-Solano et al. 2012). Furthermore, the POD for GPS and GLONASS satellites in eclipse seasons is improved because the model intrinsically accommodates the change of satellite attitude (Rodríguez-Solano et al. 2013). In this case, the orientation of the satellite bus and the SPs must be properly defined. Despite this success, the prevailing problem of the ABW model is the need to know the satellite surface areas and their optical properties. That information is currently available only for GPS, some GLONASS satellites, and the Galileo IOV satellites. Moreover, nine correlated parameters (i.e., SP, SB, Y0, +XAD, +XR, ±ZAD, and ±ZR, see Rodríguez-Solano et al. 2013) in the ABW model must be estimated for YS mode; reasonable results are achieved only with a priori constraints being put on most of those parameters. Further investigation is, therefore, required for the mutual correlation of those

estimation parameters or to identify parameter subsets and combinations that can be freely estimated if no good a priori knowledge is available.

To avoid the disadvantages of the ABW model, Montenbruck et al. (2015) reformulated the box-wing model. The deduced model employs a parameterization that isolates distinct contributions (cube, stretch, and z-asymmetry) of the satellite bus. Considering the SRP acting on SPs, the model can be expressed in  $D$  and  $B$  directions in the YS mode as follows:

$$\begin{aligned} a_D &= -a_C^{\alpha\delta} \left( |\cos \varepsilon| + \sin \varepsilon + \frac{2}{3} \right) \\ &\quad -a_S^{\alpha\delta} \left( |\cos \varepsilon| - \sin \varepsilon - \frac{4}{3} \sin^2 \varepsilon + \frac{2}{3} \right) \\ &\quad -a_A^{\alpha\delta} \left( \cos \varepsilon + \frac{2}{3} |\cos \varepsilon| \cos \varepsilon \right) \\ &\quad -2a_C^\rho \left( |\cos \varepsilon| \cos^2 \varepsilon + \sin^3 \varepsilon \right) \\ &\quad -2a_C^\rho \left( |\cos \varepsilon| \cos^2 \varepsilon - \sin^3 \varepsilon \right) - 2a_A^\rho \cos^3 \varepsilon \\ &\quad -a_{SP} \\ a_B &= -\frac{4}{3} a_S^{\alpha\delta} (\cos \varepsilon \sin \varepsilon) - \frac{2}{3} a_A^{\alpha\delta} (|\cos \varepsilon| \sin \varepsilon) \\ &\quad -2a_C^\rho ((|\cos \varepsilon| - \sin \varepsilon) \cos \varepsilon \sin \varepsilon) \\ &\quad -2a_S^\rho ((|\cos \varepsilon| + \sin \varepsilon) \cos \varepsilon \sin \varepsilon) \\ &\quad -2a_A^\rho \cos^2 \varepsilon \sin \varepsilon \end{aligned} \tag{6}$$

where  $a_{SP}$  is the acceleration induced by SPs,  $a_C^{\alpha\delta}$ ,  $a_S^{\alpha\delta}$  and  $a_A^{\alpha\delta}$  represent the effect of a cubic, stretched, and asymmetric contributions of satellite body shape related to absorption plus diffuse reflection (superscript  $\alpha\delta$ ), while  $a_C^\rho$ ,  $a_S^\rho$  and  $a_A^\rho$  are related to the specular reflection ( $\rho$ ) part for the corresponding body shape contributions, the mean value of the +Z and -Z surface is also introduced as  $a_z^{\alpha\delta}$  and  $a_z^\rho$  for  $\alpha + \delta$  and  $\rho$  to calculate the above parameters, respectively:

$$\begin{aligned} a_i^{\alpha\delta} &= \frac{A_i S_0}{M c} (\alpha_i + \delta_i) & a_i^\rho &= \frac{A_i S_0}{M c} \rho_i \\ a_z^{\alpha\delta} &= \frac{1}{2} (a_{+z}^{\alpha\delta} + a_{-z}^{\alpha\delta}) & a_z^\rho &= \frac{1}{2} (a_{+z}^\rho + a_{-z}^\rho) \\ a_C^{\alpha\delta} &= \frac{1}{2} (a_z^{\alpha\delta} + a_{+x}^{\alpha\delta}) & a_C^\rho &= \frac{1}{2} (a_z^\rho + a_{+x}^\rho), \\ a_S^{\alpha\delta} &= \frac{1}{2} (a_z^{\alpha\delta} - a_{+x}^{\alpha\delta}) & a_S^\rho &= \frac{1}{2} (a_z^\rho - a_{+x}^\rho) \\ a_A^{\alpha\delta} &= \frac{1}{2} (a_{+z}^{\alpha\delta} - a_{-z}^{\alpha\delta}) & a_A^\rho &= \frac{1}{2} (a_{+z}^\rho - a_{-z}^\rho) \end{aligned} \tag{7}$$

where  $a_i^{\alpha\delta}$  and  $a_i^\rho$  ( $i = +Z, -Z, +X$ ) are related to absorption plus diffuse reflection and reflection of the individual body surface. These parameters are calculated from the a priori geometrical (i.e.,  $A_i$ ) and physical properties (i.e.,  $M$ ,  $\alpha_i$ ,  $\delta_i$ , and  $\rho_i$ ) or estimated by fitting real measurements.

The Sun–spacecraft–Earth angle  $\varepsilon$  in Eq. (6) can be expressed as

$$\cos \varepsilon = \cos \beta \cos \mu, \quad (8)$$

where  $\mu$  is the orbit angle; i.e., the argument of satellite with respect to the midnight point, i.e., the position where the satellite is far away from the Sun in the orbit plane.

### 3 Comparison of SRP models

In this section, the performances of the ECOM1, ECOM2, and ABW models are investigated and compared. Based on the analysis of QZSS orbit consistency (i.e., OODs) and SLR residuals, the advantages and disadvantages are described and used as references to establish an a priori SRP model for the QZSS Michibiki satellite.

#### 3.1 POD strategy

The tracking data from the IGS MGEX in 2014 were collected for orbit and clock determination. The data processing was divided into two steps. First, the 3-day GPS data from MGEX tracking stations, together with the IGS final GPS orbit, the 30-s clock, and the earth rotation parameter products from the International Earth Rotation Service were used to produce a static precise point positioning (PPP) solution for each station. Second, the measurements of the QZSS from the same stations were used. The station positions, troposphere delay, and receiver clocks obtained in the previous GPS-only PPP were introduced as known parameters. The a priori orbits and clocks that originated from the broadcast ephemeris were taken as initial values. The corrections of satellite orbital parameters with respect to their initial values, satellite clock offsets, inter-system biases, and float ambiguities were estimated. The POD strategy was similar to that used in Zhao et al. (2013). With a focus on the SRP models, the attitude mode of the QZSS satellite bus presented in Ishi-

jima et al. (2008) was used directly in this study. As Michibiki is in an eccentric orbit instead of an almost circular one like other GNSSs, the one-cycle-per-revolution periodic acceleration bias induced by the Earth radiation pressure (ERP) for Michibiki would contaminate the SPR. However, the ERP was not accounted for and was left to be partly absorbed by the SRP in this contribution. Four different solutions, listed in Table 1, were determined for the QZSS Michibiki satellite.

The reasons for selecting these models were as follows: First, the C5 model has been most widely adopted for Michibiki POD. Hence, it is used as the benchmark for comparison. Second, although the C5a model could improve the orbit quality of BeiDou IGSO and MEO satellites in the ON mode, it has not been tested for QZSS POD. In this study, its performance for QZSS was validated. Third, the ECOM2 model has the ability to reduce the  $\beta$ -angle-dependent systematic orbit and clock errors in the YS mode, but it fails to represent the SRP acceleration in the ON mode, as shown in Prange et al. (2015, 2017). Hence, it helps to understand the deficiency of the C5 model in the YS mode. Fourth, the ABW model could also represent the  $\mu$ -dependent features and reduce the  $\beta$ -angle-dependent systematic error, as shown in Guo et al. (2016) for BeiDou IGSO satellites. Hence, this model was used to investigate whether the  $\beta$ -angle-dependent error could be reduced for the Michibiki satellite. In addition, this model could intrinsically accommodate the satellite attitude, so it had potential to improve the orbit in the ON mode. In this case, the orientation of the SPs in the ON mode should be carefully modeled, because SPs in general are main structures and the major contributors to the SRP perturbation.

In the ON mode, solar radiation is no longer perpendicular to the SPs. Rodríguez-Solano et al. (2013) obtained a better orbit by assuming that the SPs were as perpendicular as possible to the solar incidence direction for the satellite during yaw maneuvers. However, as analyzed in Guo et al. (2016) for BeiDou IGSO and MEO satellites, improved orbits were determined with a simple assumption: Solar radiation is still perpendicular to SPs in the ON mode. In this study, Eq. (2)

**Table 1** Solutions, SRP models used, and parameters estimated

Solution	SRP model	Estimated parameters
C5	ECOM1 without an a priori model	$D_0$ , $Y_0$ , $B_0$ , $B_{1,c}$ , and $B_{1,s}$
C5a	ECOM1 without an a priori model, but with an empirical constant acceleration bias in the along-track component ( $A_0$ )	$D_0$ , $Y_0$ , $B_0$ , $B_{1,c}$ , $B_{1,s}$ and $A_0$
D4B1	ECOM2 without an a priori model	$D_0$ , $Y_0$ , $B_0$ , $B_{1,c}$ , $B_{1,s}$ , $D_{2,c}$ , $D_{2,s}$ , $D_{4,c}$ , and $D_{4,s}$ (Arnold et al. 2015)
ABW	ABW model	SP, SB, $Y_0$ , +XAD, +ZAD, $-ZAD$ , +XR, +ZR, and $-ZR$ for the YS mode (Rodríguez-Solano et al. 2013), SP, SB, $Y_0$ , +XAD, $-XAD$ , +YAD, $-YAD$ , +ZAD, $-ZAD$ , +XR, $-XR$ , +YR, $-YR$ , +ZR, and $-ZR$ for the ON mode

**Table 2** Approximate values of optical and geometrical properties of the QZSS Michibiki bus and solar panels

Panel	Area (m <sup>2</sup> )	$\alpha$	$\rho$	$\delta$
+X/-X	17.988	0.440	0.112	0.448
+Y/-Y	19.220	0.440	0.112	0.448
+Z/-Z	8.990	0.350	0.650	0.0
Solar panels	30.0	0.720	0.196	0.034

was used to determine the DYB frame for C5, C5a, and D4B1 SRP models without regard to the actual attitude. For ABW model, the actual attitude was used for different seasons, and the satellite body-fixed frame for YS ( $\mathbf{e}_{X,YS}, \mathbf{e}_{Y,YS}, \mathbf{e}_{Z,YS}$ ) and ON ( $\mathbf{e}_{X,ON}, \mathbf{e}_{Y,ON}, \mathbf{e}_{Z,ON}$ ) could be obtained as follows:

$$\begin{aligned}
 \mathbf{e}_{X,YS} &= \mathbf{e}_{Y,YS} \times \mathbf{e}_{Z,YS} & \mathbf{e}_{Y,YS} &= \frac{\mathbf{e}_O \times \mathbf{r}}{\|\mathbf{e}_O \times \mathbf{r}\|} \\
 \mathbf{e}_{Z,YS} &= -\frac{\mathbf{r}}{\|\mathbf{r}\|} \\
 \mathbf{e}_{X,ON} &= \mathbf{e}_{Y,ON} \times \mathbf{e}_{Z,ON} & \mathbf{e}_{Y,ON} &= -\frac{\mathbf{r} \times \mathbf{v}}{\|\mathbf{r} \times \mathbf{v}\|}, \\
 \mathbf{e}_{Z,ON} &= -\frac{\mathbf{r}}{\|\mathbf{r}\|}
 \end{aligned}
 \tag{9}$$

where  $\mathbf{v}$  is the velocity of satellite.

Good knowledge of the a priori information of the satellite is essential for the ABW model. Because the information available for the geometrical and optical properties of the Michibiki satellite was limited, we adopted the approximate size of the satellite body (i.e., 2.9 m × 3.1 m × 6.1 m) and the mass (1800 kg) from IGS MGEX. For each SP, the length and width were assumed to be 7.5 m and 2 m, respectively. No public information was available on the optical properties of the satellite bus and the SPs, so we assumed an absorption of  $\alpha = 0.44$  for the multilayer insulation based on representative values in Rodríguez-Solano et al. (2012). For the SPs, the values were based on representative values for BeiDou IGSO and MEO satellites in Guo et al. (2016). The values used are listed in Table 2.

In addition, the a priori constraints being put on the parameters had a marked effect on the orbit quality determined with the ABW model. Figure 1 shows the cross-correlation for those adjustable parameters when  $\beta$  was approximately  $-60^\circ$  (a) and  $3^\circ$  (b). The SP parameter was highly correlated with the +XAD parameters in the YS mode. For both the YS and ON modes, +XAD was strongly correlated with the +XR parameters, and same for -XAD and -XR. Different from the parameters in  $\pm X$  surfaces, a high correlation existed in +ZAD and -ZAD, which showed almost no correlation with the corresponding reflection parameters in YS mode; that is, +ZR and -ZR. Once the satellite switched to the ON orientation, the correlation between SB and +ZR as well as -ZR increased from 0.3 to 0.6, and substantial variations could be observed for the estimated SB, +ZAD, and +ZR parameters when  $\beta$  was close to  $5^\circ$  (Fig.2); -ZAD and -ZR

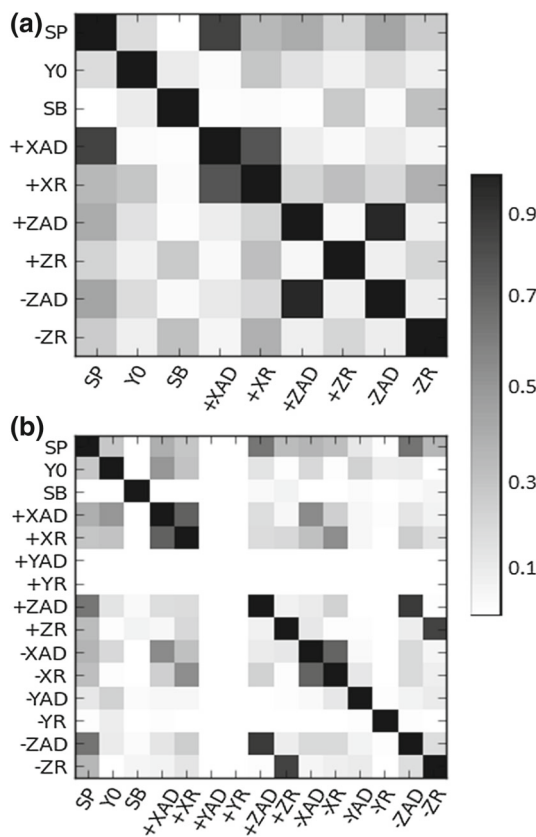


**Fig. 1** Correlations between different SRP parameters for the ABW model. **a** YS mode when  $\beta$  was approximately  $-60^\circ$ . **b** ON mode when  $\beta$  was approximately  $3^\circ$ , as the +Y surface was not illuminated, and the corresponding values were set to 0

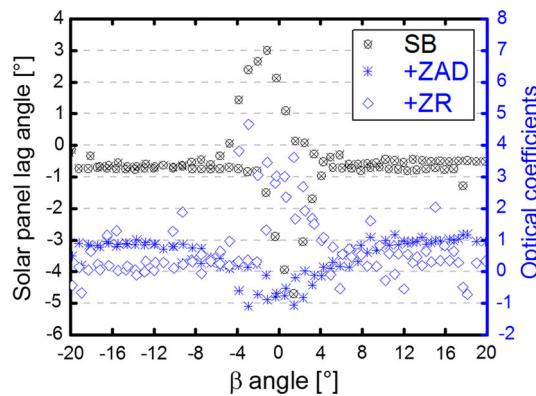


**Fig. 2** Adjusted parameters variations in the ON mode for the ABW model. The left Y axis represents SB (cross cycle), and the right Y axis is used for optical parameters [i.e., +ZAD (blue stars) and +ZR (blue diamonds)]

showed similar variations. The mean value of SB equaled  $-0.66 \pm 0.11^\circ$  for ON once the estimated values with  $\beta$  less than  $5^\circ$  were removed. Hence, in this period, the SB was tightly constrained to the mean value, and in the other case a loose-constraint (i.e., 0.1) was set for all SRP-related parameters of the ABW model because of the inaccurate a priori geometrical and optical information used.

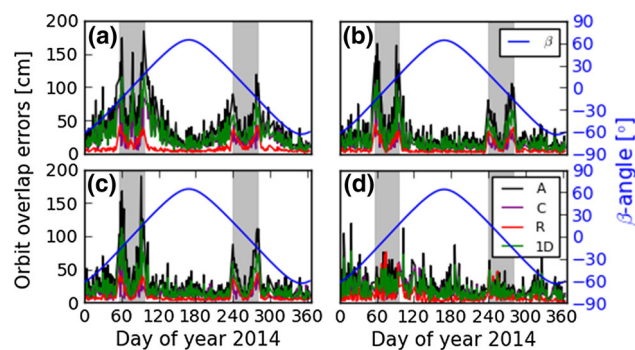


**Fig. 3** Daily RMSs of OODs in the along-track (*A*, black line), cross-track (*C*, purple line), radial (*R*, red line), and one-dimension (*1D*, green line) for **a** C5, **b** C5a, **c** D4B1, **d** ABW. The gray shade indicates the ON regimes, and the blue line represents the  $\beta$  angle

### 3.2 Orbit overlap error

The 48-h overlapping orbits of consecutive arcs are commonly used to evaluate the internal consistency of orbit solutions. Considering the two attitude modes used by the Michibiki satellite, only arcs in the same attitude mode were used for comparison. Those containing attitude-switching epochs were removed due to substantial orbit uncertainty during the period. In addition, the overlapping orbits were treated as outliers and removed once the average RMS values over the three components of the orbit differences were larger than 100 and 300 cm for arcs in the YS and ON modes, respectively. Then a 3-sigma criterion was used to exclude some outliers in the rest data. Furthermore, all four solutions on the same day were not accounted for either if one of them was detected as an outlier. The number of common solutions for all four solutions was 340.

Figure 3 illustrates the daily RMSs of OODs in the along-track (*A*), cross-track (*C*), radial (*R*), and one-dimension (*1D*) for the different SRP models. The following conclusions are drawn from this figure. First, compared with other three solutions, the C5 solution (Fig. 3a) shows the  $\beta$ -angle-dependent systematic error in the along-track and cross-track components. This clearly indicates that the C5 is deficient for modeling the SRP acting on the Michibiki satellite in the YS mode, which was also found by Prange et al. (2015). Second, once the satellite switched to the ON orientation, OODs increased no matter which kinds of SRP models were used, particularly for the C5, C5a (Fig. 3b), and D4B1 (Fig. 3c). The pronounced correlation between OODs and the  $\beta$  angle was found. The difference was at the minimum when  $\beta$  was close to zero and increased with the increase in  $\beta$  up to the threshold of the attitude switch. It demonstrates the failure of those models to represent SRP acceleration acting on the satellite in the ON mode, as ECOM models are designed for modeling SRP in YS mode. Specifically, the orbit differences are larger when the Sun is crossing the orbit plane from the

**Table 3** Statistical results for OODs of four solutions in two attitude modes (unit: cm)

Solution	YS				ON			
	A	C	R	1D	A	C	R	1D
C5	36.99	26.24	5.54	26.47	75.07	31.34	23.43	47.76
C5a	22.42	13.42	4.42	15.27	70.79	27.41	23.07	46.63
D4B1	23.46	14.33	6.42	16.37	66.28	27.08	23.51	43.82
ABW	29.46	18.47	7.60	20.88	33.62	21.55	21.95	27.36

*A* along-track, *C* cross-track, *R* radial, *1D* one-dimension

below (negative  $\beta$ -angle) to above (positive  $\beta$ -angle) compared with those when the Sun move to the opposed direction.

Table 3 lists the corresponding statistical results. In general, the four solutions show different consistencies in the YS mode. The C5a performed better than the others, followed by D4B1, and the C5 solution had the worst performance. By the introduction of a constant acceleration bias in the along-track direction in C5, the orbit consistency was markedly improved, particularly in the along-track and cross-track directions. As shown in Fig. 3, the improvement was attributable to reduced  $\beta$ -angle-dependent orbit error. This is why the D4B1 and ABW solutions also showed better consistency than that of C5. The ABW solution's performance was intermediate between those of D4B1 and C5. This could have been caused by inaccurate physical and geometrical properties used for the POD, and the use of improper constraints.

Once the Michibiki satellite switched to the ON orientation, the overlapping orbit differences increased no matter which SRP models were used. The accuracy degradation was mainly in the along-track and radial directions for C5, C5a, and D4B1, but was mainly in the radial direction for the ABW solution. This clearly indicates that the mismodeled SRP perturbation mainly affects these directions. Among the four solutions, the ABW solution showed the best performance, which degraded only slightly (from 20.9 to 27.4 cm in 1D) compared to the result in YS mode; this can be attributed to the reduced  $\beta$ -dependent systematic error, especially for the along-track direction (see Fig. 3), and the other three models showed similar performance (47.8, 46.6, and 43.8 cm for C5, C5a, and D4B1 in the 1D direction, respectively).

Although the C5a solution showed the best performance for BeiDou IGSO and MEO satellites in the ON mode (Guo et al. 2016), that model is not suitable for the QZSS Michibiki satellite, as shown here. We believe that the reason for this is that the threshold for the attitude switch is approximately  $4^\circ$  for the BeiDou IGSO and MEO satellites, instead of approximately  $20^\circ$  for the Michibiki satellite. The relatively lower threshold angle of the BeiDou IGSO and MEO satellites allows the mismodeled SRP perturbation to be easily absorbed by the introduced constant bias in the along-track. However, this may not be the case for the Michibiki satellite.

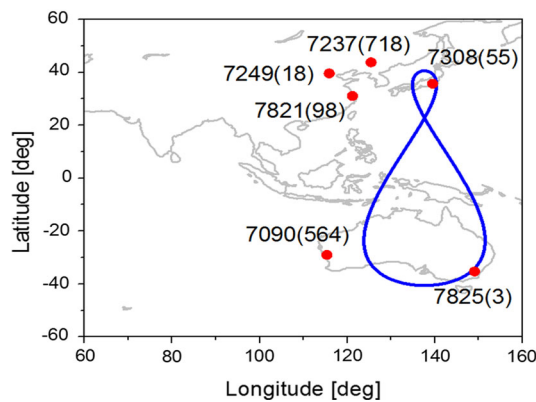


**Fig. 4** Distribution of SLR stations (red dots) and numbers of used NPs (in parentheses). The blue line represents the ground footprint of the QZSS Michibiki satellite

In addition, it is interesting to note that the consistency of D4B1 was slightly better than that of C5a, even though the C5a solution showed the best consistency in the YS mode. The reasons are that, on the one hand, the C5a model is not good enough for QZSS POD in the ON mode; on the other hand, the D4B1 model has three more parameters that may fit the measurements better.

### 3.3 SLR validation

As previously mentioned, the QZSS Michibiki satellite carries a LRA, which allows its orbits computed from GNSS observations to be assessed independently with SLR measurements. Predominantly, SLR residuals are an indicator of the radial accuracy of GNSS orbits, because the maximum incidence angle of a laser pulse to a QZSS satellite (nadir angle) is only approximately  $9^\circ$ . We collected 1456 SLR normal points (NPs) from ILRS (Pearlman et al. 2002) in 2014. More than 86% of the data were provided by stations 7237 (Changchun, China) and 7090 (Yarragadee, Australia). Figure 4 shows the station distribution and number of used NPs for each station. The solutions containing attitude switch epochs were not considered in the statistics. The orbits in the middle day of the 72-h POD arc were used for validation. SLR residuals exceeding an absolute value of 100 cm and 300 cm in the YS and ON modes, respectively, were excluded from validation. Afterward, data with value larger than 3-sigma were also excluded in the rest of the SLR residual series. As a result, the numbers of excluded data are 7 and 9 for the YS and ON modes, respectively. The SLR validation results are listed in Table 4.

For orbits in the YS mode, the ABW solution showed the best performance (RMS 9.2 cm), and the standard deviation (STD) was 8.5 cm with a  $-3.6$  cm bias. A 10–20 cm accuracy (RMS) was achieved for other three solutions. Among them, the C5a solution showed the largest STD (20.3 cm) and

**Table 4** SLR statistical results for four solutions in the YS and ON modes (unit: cm)

Solution	YS			ON		
	Bias	STD	RMS	Bias	STD	RMS
C5	-5.3	16.1	17.0	14.7	48.3	50.4
C5a	0.4	20.3	20.3	31.3	38.0	49.2
D4B1	-12.4	7.1	14.3	24.5	42.3	48.9
ABW	-3.6	8.5	9.2	4.6	32.7	33.0

smallest bias (0.4 cm), although it had the best performance in OODs. The C5 solution had the worst consistency, but its SLR validation precision was better than that of the C5a solution. However, there was a relatively large bias in the C5 solution ( $-5.3$  cm). The D4B1 solution showed the largest negative bias ( $-12.4$  cm) with the smallest STD (7.1 cm) in the SLR residuals. Once the satellite switched to the ON orientation, a marked degradation of orbit quality was identified by SLR residuals for all solutions. In general, a positive bias was found for all four SRP models: The ABW solution showed the best performance again with the smallest bias and STD. The accuracy of the other three solutions was almost the same and reached approximately 50 cm. The observed mean bias in SLR residuals indicates that there were unmodeled accelerations.

Furthermore, we analyzed the SLR residuals against  $\beta$  and  $\mu$  angles. Figure 5 demonstrates the one-way SLR residuals for the C5 (Fig. 5a), C5a (Fig. 5b), D4B1 (Fig. 5c), and ABW (Fig. 5d) solutions. In each subfigure, the upper left and right panels show residuals against  $\beta$  only and against both  $\beta$  and  $\mu$ , respectively, whereas the lower right panel shows the residuals against  $\mu$  only. The fitted variations of SLR residuals against  $\beta$  or  $\mu$  are shown in the upper left or lower right panel by the black line. Particularly, in the lower right panel, the black line with a circle at the end is the fitted variation of SLR residuals in YS regime, whereas the line with a triangle is for the ON. It is clear that the C5 and C5a solutions had pronounced  $\beta$ -angle-dependent orbit error. It was reduced partially in the D4B1 solution and almost completely eliminated in the ABW solution. As recognized from the fitted line for residuals against the  $\mu$  angle, orbit angle-dependent systematic error for C5 and C5a existed in the SLR residuals whether the satellite was in the YS or ON mode. This systematic error was eliminated substantially for the D4B1 and ABW solutions when the satellite was in the YS season. Moreover, it was much reduced in the ABW solution for the ON period.

Based on the above analysis of OODs and SLR residuals of these four solutions, the following conclusions can be made



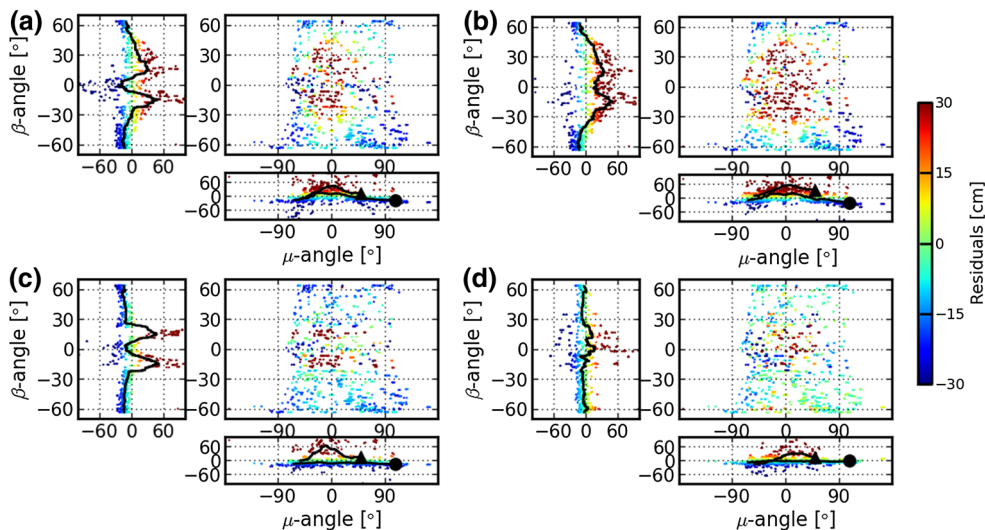


**Fig. 5** One-way SLR residuals for **a** C5, **b** C5a, **c** D4B1, and **d** ABW solutions (the *black line with a circle at the end* is the fitted variation of SLR residuals using a moving average for the YS season. The *black line with a triangle* is for the ON season.)

and used as a reference for the establishment of an a priori model for the QZSS Michibiki satellite:

- For POD in the YS mode, the OODs and SLR residuals of the C5 solution show clear  $\beta$ -angle-dependent systematic error, and the error in overlapping orbits could be reduced with additional parameters adjusted (i.e., C5a and D4B1). However, the systematic errors in SLR residuals could not be eliminated completely for D4B1 and even be amplified for C5a solution. Although the C5a and D4B1 solutions show better consistency than that of ABW, the performance in the SLR validation of the ABW model is more promising, which can be attributed to the significant reduction of  $\beta$ -angle-dependent systematic error by this model.
- For POD in the ON mode, C5, C5a, and D4B1 fail to represent the real SRP acting on the QZSS Michibiki satellite. The OODs of those solutions show clear  $\beta$ -angle dependence, particularly in the along-track and radial directions. The errors are also found in SLR residuals, whereas the ABW can reduce systematic errors, although inaccurate geometrical and optical information is adopted in the model.

Hence, as the analytical model, the ABW model could capture the short-periodic SRP perturbations to remove the  $\beta$ -angle dependence orbit error and adapt to the changes of attitude, to achieve better orbit in ON mode. In addition, as the empirical model, ECOM could fit the measurements quite well to obtain orbits with better consistency. Considering the different performances of the ABW model and the ECOMs, it is possible to establish a better SRP model for the Michibiki satellite by combining the ECOM and ABW models.

### 4 Enhanced SRP model for Michibiki satellite

With the above considerations, the parameters of an a priori SRP model can be obtained from ABW model to augment the purely ECOM. Furthermore, the enhanced SRP model will also be validated by orbit consistency (i.e., OODs) and SLR measurements, as well as the variation of SRP parameters.

#### 4.1 Establishment of the a priori model

As the SPs are not perpendicular to the Sun radiation in the ON mode, the DYB frame defined in Eq. (2) is not the best accounts for the SPs orientation to describe the SRP acceleration. Hence, the DYB for ON mode is introduced and spanned by the three unit vectors ( $\mathbf{e}_{D,ON}$ ,  $\mathbf{e}_{Y,ON}$ , and  $\mathbf{e}_{B,ON}$ ):

$$\begin{aligned} \mathbf{e}_{D,ON} &= \mathbf{e}_{Y,ON} \times \mathbf{e}_{B,ON} \\ \mathbf{e}_{Y,ON} &= -\frac{\mathbf{r} \times \mathbf{v}}{\|\mathbf{r} \times \mathbf{v}\|} \\ \mathbf{e}_{B,ON} &= \mathbf{e}_{\odot} \times \mathbf{e}_{Y,ON} \end{aligned} \tag{10}$$

In general, two steps were used to establish the a priori model for QZSS Michibiki satellite. First, the optical parameters of satellite solar panels and buses were estimated from the ABW solution with 2014 data, and Fig. 6 shows their dependency on the  $|\beta|$ -angle. It is clear that all the parameters vary between  $-0.1$  and  $2.0$  and indicates that ABW can model SRP perturbation quite well in both YS and ON modes. The median of SP is  $1.23$  and the corresponding acceleration ( $a_{SP}$ ) caused by SPs is approximately  $93.5 \text{ nm/s}^2$ . The median values of absorption plus diffuse reflection ( $\alpha + \delta$ ) were  $0.88$ ,  $0.66$ , and  $0.52$  for  $+X$ ,  $+Z$  and  $-Z$  surface, respectively, and the corresponding medians were  $0.01$ ,  $0.28$ , and  $0.36$  for

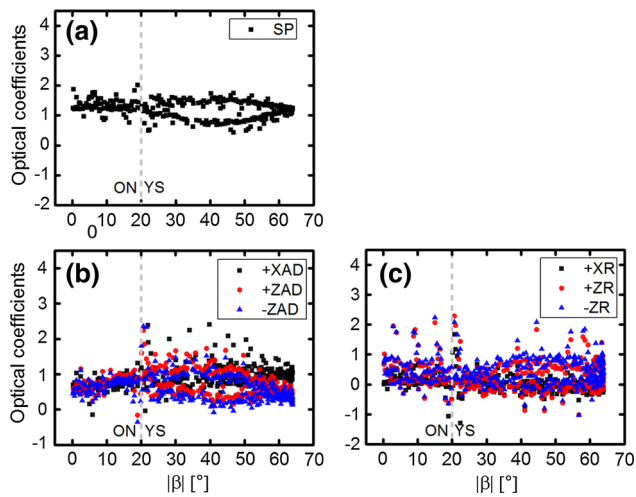


**Fig. 6** Variation of the optical parameters of Michibiki calibrated from the ABW solution with respect to  $|\beta|$ , **a** SP; **b** absorption plus diffuse reflection; **c** specularly reflected photons. The a priori areas for each surface used in ABW solution are listed in Table 2

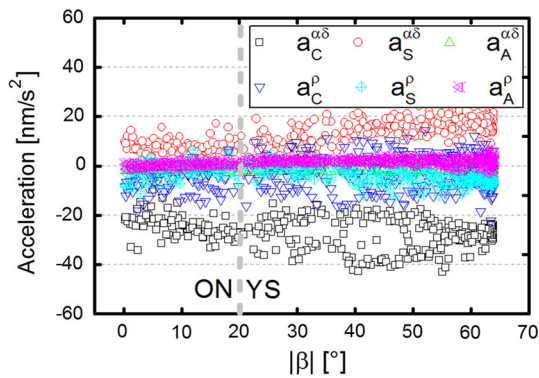


**Fig. 7** Variations of the SRP acceleration of the cubic, stretched, and asymmetric contributions of satellite body shape related to absorption plus diffuse reflection and the specular reflection part in Eq. (7) with respect to  $|\beta|$

the specularly reflected photons ( $\rho$ ). Considering the inaccurate areas used, we did not set the high constrain (i.e.,  $\alpha + \delta + \rho = 1$ ) for ABW solution. As a result, the sum of absorption, diffuse reflection, and specular reflection does not equal to one.

The SRP acceleration of the cubic, stretched, and asymmetric contributions of satellite body shape related to absorption plus diffuse reflection and the specular reflection part in Eq. (7) can be obtained, and Fig. 7 illustrates their variations with dependency on the  $|\beta|$ -angle. It can be seen that the variations of all parameters are quite stable. The maximum slope is approximately 0.2 for  $a_C^\rho$ , and the slopes are less than 0.1 for others. With the estimated  $a_{SP}$ ,  $a_C^i$ ,  $a_S^i$  and  $a_A^i$  ( $i = \alpha\delta, \rho$ ), the SRP acceleration contributed by satellite SPs and buses can be obtained by Eq. (6).

The perturbations induced by the Y surfaces, which are illuminated by solar radiation in the ON mode, have not been

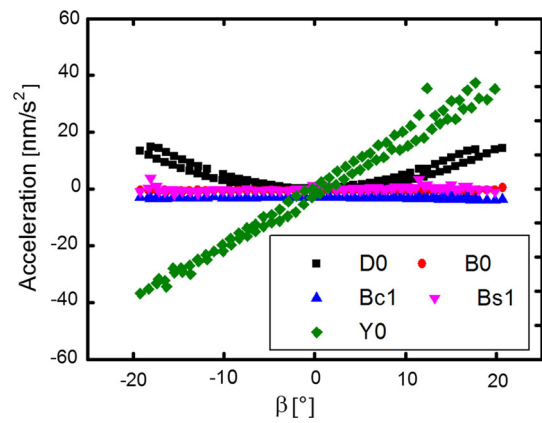


**Fig. 8** Estimated SRP parameters with the a priori model expressed in Eq. (6) when the satellite was in the ON mode

accounted for in Eq. (6). Hence, in the second step, refinement was required to compensate for the remaining modeling deficiency in the ON mode. To achieve this, the QZSS Michibiki orbits were redetermined in the second step with the a priori model originated from Eq. (6) and the redefined DYB frame in Eq. (10), and the estimated five parameters of the reformulated ECOM were investigated. Clear  $\beta$ -angle-dependence for D0 is shown in Fig. 8. As the SPs' contribution was already considered in Eq. (6), the estimated D0 reached zero when the Sun was close to satellite orbital plane. Moreover, a marked linear variation of Y0 is also evident; it indicates that the modeling deficiencies are mainly in both D and Y directions. To model them, we fitted these parameters with the 2-order polynomial against the  $\beta$ -angle in radian as follows:

$$\begin{aligned} a_D^{ON} &= a_D + a_{D0}^{fit} \\ a_B^{ON} &= a_B + a_{B0}^{fit} \\ a_Y^{ON} &= a_{Y0}^{fit} \\ a_*^{fit} &= a_{*,0} + a_{*,1}\beta + a_{*,2}\beta^2 \end{aligned} \quad (11)$$

where  $a_D$  and  $a_B$  can be obtained with Eq. (6) with orientation defined in Eq. (10), the median values of corresponding coefficients are listed in Table 5, and  $a_{*,0}$ ,  $a_{*,1}$ , and  $a_{*,2}$  are the parameters to be fitted for  $a_{D0}^{fit}$ ,  $a_{B0}^{fit}$ , and  $a_{Y0}^{fit}$ . Extensive tests indicate that only a linear equation is sufficient to represent the unmodeled perturbations in the Y direction, whereas the constant term and first-order can be omitted for the  $D_0$  component. However, a noise bias (approximately  $-3 \text{ nm/s}^2$ ) must be modeled for the  $B_{1,c}$  component. Hence, only three parameters,  $a_{D0,2}$ ,  $a_{B_{1,c},0}$  and  $a_{Y0,1}$ , are required for modeling the perturbation. All the coefficients used in the a priori model are listed in Table 5.

**Table 5** Estimated parameters of the a priori SRP model expressed in Eqs. (6) and (11) for the QZSS Michibiki satellite (unit:  $\text{nm}/\text{s}^2$ )

Coefficient	YS/ON	Coefficient	ON
$a_C^{\alpha\delta}$	26.9	$a_{D_{0,2}}$	128.5
$a_S^{\alpha\delta}$	-13.0	$a_{Y_{0,1}}$	109.0
$a_A^{\alpha\delta}$	1.6	$a_{B_{1,c,0}}$	-3.0
$a_C^\rho$	3.3	-	-
$a_S^\rho$	3.8	-	-
$a_A^\rho$	-1.5	-	-
$a_{SP}$	93.5	-	-

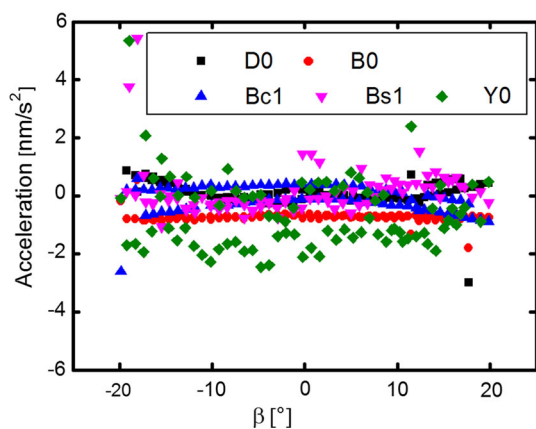


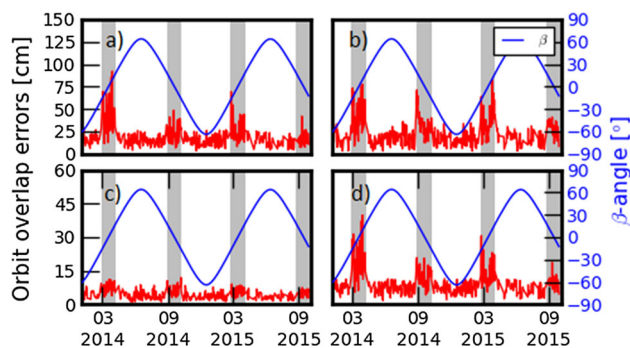
**Fig. 9** Estimated ECOM parameters in 2014 with the a priori model expressed in Eq. (11) when the satellite was in the ON mode

### 4.2 Model validation

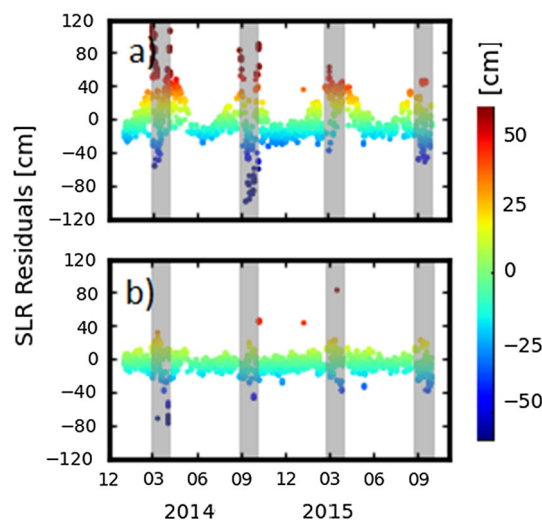
To assess the performance of the proposed a priori SRP model, both OODs and SLR residuals were used as metrics for assessing internal consistency and accuracy. In addition, the time series of the five estimated parameters of the ECOM were also taken into account.

Figure 9 shows the variations of estimated ECOM parameters with the proposed a priori model when the satellite was in the period of the ON mode in 2014. As expected, no obvious  $\beta$ -angle-dependence variation was found for the parameters, which indicates clearly that the systematic orbit error was compensated for.

Because the data in 2014 were used to establish the a priori SRP model, the data in the first 9 months of 2015 were used to assess the performance of the proposed a priori SRP model. Figure 10 shows the corresponding daily RMS of OODs in the along-track, cross-track, and radial directions and the one-dimension (1D). Compared with that shown in Fig. 3a, substantial improvement is visible for overlapping orbits in the ON mode. The  $\beta$ -angle-dependent error in the selected period was almost completely reduced, particularly for the radial direction, and the averaged RMSs were approx-



**Fig. 10** Daily RMSs of OODs for the solution determined with enhanced SRP model. **a** Along-track. **b** Cross-track. **c** Radial. **d** 1D. The blue line represents  $\beta$  angle. The gray shaded areas indicate the ON seasons



**Fig. 11** One-way SLR residuals for the C5 (a) and enhanced solution (b). The gray shaded areas indicate the ON seasons

imately 29.4, 22.3, and 6.4 cm in the along-track, cross-track, and radial directions, respectively. For the YS mode, the average RMSs were approximately 15.6, 10.5, and 4.0 cm for along-track, cross-track, and radial directions, respectively.

Furthermore, 2426 NPs over the period were collected from the ILRS. Figure 11 shows the SLR residuals for the C5 (Fig. 11a) in Table 1 and the solution determined with the proposed a priori model (enhanced solution) (Fig. 11b) in the selected period. It can be seen that the  $\beta$ -dependent systematic error was almost completely eliminated in the YS mode. In addition, the larger SLR residuals in the ON mode were also reduced, and the residuals become smaller and more stable.

Table 6 lists the corresponding statistical results. Compared with the C5 solution, better accuracy was achieved for the solution determined with the enhanced solution. In 2014, orbit accuracy was improved to approximately 7.9 cm and 15.2 cm in the YS and ON modes, respectively. Similar

**Table 6** SLR statistical results for the C5 solution and enhanced solution, respectively (unit: cm)

Solution	Year	YS			ON		
		Bias	STD	RMS	Bias	STD	RMS
C5	2014	-5.3	16.1	17.0	14.7	48.3	50.5
	2015	-3.4	13.2	13.6	4.4	26.6	27.0
Enhanced solution	2014	-5.1	6.1	7.9	-2.0	15.1	15.2
	2015	-4.2	6.0	7.3	-5.4	13.9	14.9

improvement could also be observed for orbits in 2015. However, there is still a negative bias in the YS mode that is partly caused by the unmodeled perturbations; that is, antenna thrust force and ERP. Although the a priori model was used, the orbit accuracy in the ON mode was still lower than that of the YS mode. This means that there is still room to improve the SRP model for Michibiki in the ON mode.

## 5 Summary and conclusion

Similar to Galileo satellites, deficiencies of the ECOM and ECOM1 in the POD of QZSS satellites have been identified by Prange et al. (2015) and confirmed by this contribution, and the limitations have become apparent. First, the two ECOM models fail to properly describe the acceleration acting on a non-cuboid body with a large area-to-mass ratio. Second, they are insufficient to describe the acceleration when the satellite is in a non-yaw-steering attitude. It is therefore imperative to improve the SRP model.

By comparing the four SRP models, we found that the C5a and D4B1 models showed better consistency in the YS regime, but SLR validation results of C5a showed larger  $\beta$ -angle-dependent errors. Although the  $\beta$ -angle-dependent errors in SLR can be reduced by D4B1, there are was a larger bias. Fortunately, the ABW model can reduce these systematic errors in SLR residuals for both YS and ON modes with a small bias, even though the determined orbits have lower consistency. Currently, due to lack of accurate geometrical and optical information, it is not possible to construct a precise analytical model for the QZSS and prompts us to establish a better SRP model by combining the ECOM and ABW models.

Hence, after defining the DYB frame for YS and ON with Eqs. (2) and (10), respectively, we established an a priori model. Generally, two steps were taken for its establishment. First, based on optical parameters from the ABW solution and areas listed in Tables 2, 6 coefficients related to satellite buses were derived by Eq. (7), and the acceleration of SPs can be computed by Eq. (4). As the perturbation introduced by the  $Y$  surfaces in the ON season was not accounted for in Eq. (6), further compensation was done for the ON

mode in the second step. Three additional parameters were used to describe the parabolic, linear, and constant accelerations perturbed in the  $D$ ,  $Y$ , and  $B$  components. In summary, the a priori model was established and used with the form expressed by Eqs. (6) and (11) for YS and ON, respectively. The coefficients listed in Table 5 are proposed for the a priori model. The definition of DYB frame for the a priori model as well as the ECOM can be obtained by Eqs. (2) and (10) for YS and ON, respectively.

By augmenting the ECOM with the new a priori model, significantly improved orbit solutions were obtained. For satellites in the YS mode, the  $\beta$ -angle-dependent error was almost eliminated, and the orbit accuracy was better than 8 cm by SLR validation. The SLR validation results in the ON mode show that the improvement was 2 times as great with the data in 2015 that were not used for establishment of the a priori model. In particular, the  $\beta$ -angle-dependent errors in overlapping orbits were also reduced. However, the negative bias still exists in the SLR validation and needs more study.

**Acknowledgements** The IGS MGEX, iGMAS, and ILRS are greatly acknowledged for providing the multi-GNSS and SLR tracking data. The research is partially supported by the National Natural Science Foundation of China (Grant Nos. 41404032, 41504009, 41574030, 41574027). Finally, the authors are also grateful for the comments and remarks of reviewers and editor-in-chief, who helped to improve the manuscript significantly.

## References

- Akiyama K, Otsubo T (2012) Accuracy evaluation of QZSS-1 orbit solutions with satellite laser ranging. International technical laser workshop 2012 (ITLW-12), 05–09 November 2012, Rome, Italy
- Arnold D, Meindl M, Beutler G, Dach R, Schaer S, Lutz S, Prange L, Sošnica K, Mervart L, Jäggi A (2015) CODE's new solar radiation pressure model for GNSS orbit determination. *J Geod* 89(8):775–791. doi:10.1007/s00190-015-0814-4
- Bar-Sever Y, Kuang D (2004) New empirically derived solar radiation pressure model for global positioning system satellites. The interplanetary network progress report, pp 42–159
- Bar-Sever Y, Kuang D (2005) New empirically derived solar radiation pressure model for global positioning system satellites during eclipse seasons. The interplanetary network progress report, pp 42–160
- Beutler G, Brockmann E, Gurtner W, Hugentobler U, Mervart L, Rothacher M, Verdun A (1994) Extended orbit modeling techniques at the CODE processing center of the international GPS service for geodynamics (IGS): theory and initial results. *Manuscr Geod* 19(6):367–386
- Dow J, Neilan R, Rizos C (2009) The International GNSS Service in a changing landscape of global navigation satellite systems. *J Geod* 83(3–4):191–198. doi:10.1007/s00190-008-0300-3
- Fliegel H, Gallini T, Swift E (1992) Global positioning system radiation force model for geodetic applications. *J Geophys Res* 97(B1):559–568. doi:10.1029/91JB02564
- Fliegel H, Gallini T (1996) Solar force modeling of block IIR global positioning system satellites. *J Spacecr Rockets* 33(6):863–866. doi:10.2514/3.26851

- Guo J, Zhao Q, Geng T, Su X, Liu J (2013) Precise orbit determination for COMPASS IGSO satellites during yaw maneuvers, vol III. In: Sun J, Jiao W, Wu H, Shi C (eds) Proceedings of China satellite navigation conference (CSNC) 2013, vol 245. Springer, pp 41–53. doi:[10.1007/978-3-642-37407-4\\_4](https://doi.org/10.1007/978-3-642-37407-4_4)
- Guo J, Chen G, Zhao Q, Wang C, Liu J, Liu X (2016) Comparison of solar radiation pressure models for BDS IGSO and MEO satellites with emphasis on improving orbit quality. *GPS Solut*. doi:[10.1007/s10291-016-0540-2](https://doi.org/10.1007/s10291-016-0540-2)
- Garcia-Serrano C, Agrotis L, Dilssner F, Feltens J, van Kints M, Romero I, Springer T, Enderle W (2014) The ESA/ESCO analysis center progress and improvements. IGS Workshop 2014, 23–27 June 2014, Pasadena, USA
- Hauschild A, Steigenberger P, Rodriguez-Solano C (2012) Signal, orbit and attitude analysis of Japan's first QZSS satellite Michibiki. *GPS Solut* 16:127–133. doi:[10.1007/s10291-011-0245-5](https://doi.org/10.1007/s10291-011-0245-5)
- Ikari S, Ebinuma T, Funase R, Nakasuka S (2013) An evaluation of solar radiation pressure models for QZS-1 precise orbit determination. In: Proceeding of the 26th international technical meeting of the satellite division of the institute of navigation (ION GNSS+ 2013), 16–20 September, 2013, Nashville, TN, USA
- Ishijima Y, Inaba N, Matsumoto A, Terada K, Yonechi H, Ebisutani H, Ukawa S, Okamoto T (2008). Design and Development of the first Quasi-Zenith Satellite attitude and orbit control system. Aerospace conference, 2009 IEEE. doi:[10.1109/AERO.2009.4839537](https://doi.org/10.1109/AERO.2009.4839537)
- Inaba N, Matsumoto A, Hase H, Kogure S, Sawabe M, Terada K (2009) Design concept of Quasi Zenith Satellite System. *Acta Astronaut* 65(7–8):1068–1075. doi:[10.1016/j.actaastro.2009.03.068](https://doi.org/10.1016/j.actaastro.2009.03.068)
- Marshall J, Luthcke S (1994) Modeling radiation forces acting on TOPEX/Poseidon for precision orbit determination. *J Spacecr Rockets* 31:99–105. doi:[10.2514/3.26408](https://doi.org/10.2514/3.26408)
- Meindl M, Beutler G, Thaller D, Jäggi A, Dach R (2013) Geocenter coordinates estimated from GNSS data as viewed by perturbation theory. *Adv Space Res* 51(7):1047–1064. doi:[10.1016/j.asr.2012.10.026](https://doi.org/10.1016/j.asr.2012.10.026)
- Milani A, Nobili AM, Farinella P (1987) Non-gravitational perturbations and satellite geodesy. *Ciel Terre* 103:128
- Montenbruck O, Steigenberger P, Khachikyan R, Weber G, Langley R, Mervart L, Hugentobler U (2014) IGS-MGEX preparing the ground for multi-constellation GNSS science. *Espace* 9(1):42–49
- Montenbruck O, Steigenberger P, Hugentobler U (2015) Enhanced solar radiation pressure modeling for Galileo satellites. *J Geod* 89(3):283–297. doi:[10.1007/s00190-014-0774-0](https://doi.org/10.1007/s00190-014-0774-0)
- Pearlman M, Degnan J, Bosworth J (2002) The international laser ranging service. *Adv Space Res* 30(2):135–143. doi:[10.1016/S0273-1177\(02\)00277-6](https://doi.org/10.1016/S0273-1177(02)00277-6)
- Prange L, Orliac E, Dach R, Arnold D, Beutler G, Schaer S, Jäggi A (2015) CODE's multi-GNSS orbit and clock solution. In: EGU General Assembly 2015, 12–17 April 2015, Vienna, Austria
- Prange L, Orliac E, Dach R, Arnold D, Beutler G, Schaer S, Jäggi A (2017) CODE's five-system orbit and clock solution—the challenges of multi-GNSS data analysis. *J Geod* 91:345. doi:[10.1007/s00190-016-0968-8](https://doi.org/10.1007/s00190-016-0968-8)
- Rodríguez-Solano C, Hugentobler U, Steigenberger P (2012) Adjustable box-wing model for solar radiation pressure impacting GPS satellites. *Adv Space Res* 49:1113–1128. doi:[10.1016/j.asr.2012.01.016](https://doi.org/10.1016/j.asr.2012.01.016)
- Rodríguez-Solano C, Hugentobler U, Steigenberger P, Allende-Alba G (2013) Improving the orbits of GPS block IIA satellites during eclipse seasons. *Adv Space Res* 52(8):1511–1529. doi:[10.1016/j.asr.2013.07.013](https://doi.org/10.1016/j.asr.2013.07.013)
- Rodríguez-Solano C, Hugentobler U, Steigenberger P, Blossfeld M, Fritsche M (2014) Reducing the draconitic errors in GNSS geodetic products. *J Geod* 88:559–574. doi:[10.1007/s00190-014-0704-1](https://doi.org/10.1007/s00190-014-0704-1)
- Springer T, Beutler G, Rothacher M (1999) A new solar radiation pressure model for GPS satellites. *GPS Solut* 2(3):50–62. doi:[10.1007/PL00012757](https://doi.org/10.1007/PL00012757)
- Steigenberger P, Hauschild A, Montenbruck O, Rodriguez-Solano C, Hugentobler U (2013) Orbit and clock determination of QZS-1 based on the CONGO network. *J Navig* 60(1):31–40. doi:[10.1002/navi.27](https://doi.org/10.1002/navi.27)
- Steigenberger P, Kogure S (2014) IGS-MGEX: QZSS orbit and clock determination. IGS Workshop 2014, 23–27 June 2014, Pasadena, USA
- Takasu T (2013) Development of multi-GNSS orbit and clock determination software “MADOCA”. The 5th Asia Oceania Regional Workshop on GNSS, December 1–3, 2013
- Zhao Q, Guo J, Li M, Qu L, Hu Z, Shi C, Liu J (2013) Initial results of precise orbit and clock determination for COMPASS navigation satellite system. *J Geod* 87:475–486. doi:[10.1007/s00190-013-0622-7](https://doi.org/10.1007/s00190-013-0622-7)